

Finite element investigation of the joints in precast concrete pavement

Vahid Sadeghi^a and Saeid Hesami*

Babol Noshirvani University of Technology, Babol, Iran

(Received March 11, 2017, Revised January 24, 2018, Accepted January 28, 2018)

Abstract. This paper measures the mechanical response of precast pavement joints under moving axle loads using the finite-element method, and the models were validated with results of field tests. In order to increase the ability to use the non-linear FE analysis for design and assessment of precast pavement subjected to moving axle load, this paper investigated the effects of different load transfer between the slabs using the ABAQUS finite-element package to solve the nonlinear explicit model equations. The assembly of the panels using dowels and groove-tongue keys has been studied to assess the efficiency of keyway joint system. Concrete damage plasticity model was used to calculate the effects of permanent damages related to the failure mechanisms. With aggregate interlock as the only load transferring system, Load transfer efficiency (LTE) is not acceptable when the axle load reaches to slab joints. The Finite-element modelling (FEM) results showed that keyway joints significantly reduced tensile stresses developed at the mid-slab. Increasing the thickness of the tongue the LTE was improved but with increasing the height of the tongue the LTE was decreased. Stresses are transferred to the adjacent slab efficiently when dowels are embedded within the model. When the axle load approaches joints, tensile damage occurs sooner than compressive damage, but the damage rate remains constant, then compressive damage increases significantly and become the major form of distress under the dowels.

Keywords: precast pavement; load transfer efficiency; concrete damage plasticity; finite element method

1. Introduction

Pavement rehabilitation in urban areas has become a critical challenge for highway agencies due to traffic disruption by increasing number of automobiles. To minimize the impacts of closure of the roadways due to overlays or replacements of the deteriorated concrete slabs, precast concrete pavements have been introduced as an effective strategy to mitigate the user costs in traffic congestion. PCPs are concrete slabs, prestressed and non-prestressed, prefabricated off-site, transported and laid on the prepared subgrade or existing pavement, which has clear advantages over conventional pavements, including better concrete because of the quality control and appropriate curing condition offsite, placement of the concrete slabs regardless of the weather condition and reduced delay to be opened to traffic (Nejad *et al.* 2013, Tayabji *et al.* 2013, Peng *et al.* 2014). These systems have been experimented in the US since early 2000s (Merritt 2000, Priddy *et al.* 2014). The use of precast concrete pavement (PCP) technology was adopted by several US highway agencies in recent years, including California DOT, Florida DOT New Jersey DOT and Utah DOT (Littleton and Mallela 2014, Tayabji 2015). Pavement repairs using PCP can be classified in two methods, full-depth repairs to repair deteriorated localized area of the

slab, and full-panel replacement (Tayabji and Hall 2008). With respect to load transfer provisions, dowel bars can be either inserted in the panel or the existing pavement, and the slots for the dowels are cut in the slab or pavement. Reconstruction or overlay on the existing pavement can be performed using PCP (Sadeghi and Hesami 2017).

Apart from the dowels, the other mechanism for connecting intermediate joints is tongue-and-groove keyway connections between panels, which is also used in U.S. developed PCP systems. The panel on one side of the joint has the keyway tongue and the panel on the other side has the keyway groove. There are a few literature regarding the application of the keyway system in the literature. In the Missouri I-57 PPCP demonstration project, constructed during December 2005, the deflection of the keyway joints under the 40 kN load was investigated. The result showed that the deflection was high, and the load transfer was low when there wasn't adequate residual prestress at the midsection (Gopalaratnam *et al.* 2007). It has been also shown that when the full depth of the keyway is not bonded tightly, the load transfer between the slabs decreased drastically. Keyed joints have also been used in the hexagonal PCPs developed in the France (de Larrard *et al.* 2013). In a study on the PCP system in Nantes, France; the effects of interlocking between the slab using keyway joint were investigated and performed successful compared to mechanically independent slabs. Their study also shown that the keyway and the base support were effective on the load transfer between the slabs.

PCP technology has been implemented recently, and the information on PCP performance is not well documented, so the technology was not fully embraced (Ashtiani and De

*Corresponding author, Associate Professor
E-mail: S.Hesami@nit.ac.ir

^aPh.D. Candidate
E-mail: Sadeghi@stu.nit.ac.ir

Haro 2016). Finite element modelling (FEM) can be utilized to explore complicated effects and interactions and assessing stresses and strains in the concrete pavement. FEM is a common computer-based method used to design and study different types of pavements and concrete slabs (Smadi and Belakhdar 2007, Mokhtatar *et al.* 2013). 3D-FEM have been used by many researchers to study dowel bars at joints of concrete pavements (Channakeshava *et al.* 1993, Abo-Qudais and Al-Qadi 2000, William and Shoukry 2001, Shoukry *et al.* 2002, Kim and Hjelmstad 2003, Hesami and Sadeghi 2015). In previous studies load transfer by aggregate interlock in transverse joints were modeled using shear spring elements or classical frictional behavior. This approximation does not simulate actual behavior of aggregate interlock. In addition, previous 3D FEMs studied the dynamic effect of the moving loads on pavements using the superposition principle or considering the load as a group of impacts with a fixed distance and velocity with linear or non-linear shapes.

There exists a limited number of FEM studies of precast panels for pavement in the literature. The effects of dowels within the precast concrete pavements has been investigated by a few researchers. Priddy *et al.* investigated the precast pavement under static loads and showed that high stress concentrations occurred in the dowel slot and suggested some modification for dowel bars (Priddy *et al.* 2014).

The assembly of the panels using dowels and groove-tongue keys has been investigated using finite element. In order to increase the ability to use the non-linear FE analysis for design and assessment of precast pavement subjected to moving axle load, this paper investigated the effects of different load transfer between the slabs using the ABAQUS finite-element package to solve the nonlinear explicit model equations. Abaqus (version 6.13) was preferred for this study because of its prevalent use for modelling concrete pavements and its built-in concrete damage models.

1.1 Concrete damaged plasticity

The nonlinear analysis of concrete in ABAQUS is mostly by using smeared crack or damaged plasticity approach. The smeared crack model is intended where concrete is subjected to essentially monotonic straining and a material point shows either tensile cracking or compressive crushing at low confining pressures. The concrete damaged plasticity model is available in ABAQUS to calculate the effects of permanent damages related to the failure mechanisms. Concrete Damage Plasticity model (CDP) is very versatile and capable of predicting the behavior of concrete structures subjected to monotonic, cyclic and dynamic loading. It assumes two main failure mechanisms, i.e., tensile cracking and compressive crushing of the concrete material. In the CDP damage model used in this study, the degradation of stresses is reflected. The Changing of the elastic stiffness to a lower state is described by two tensile and compressive damage variables, d_t and d_c , which are assumed to be functions of the plastic strains, temperature, and field variables.

The damage variables can take values from zero, for the undamaged material, to one, which represents a total loss of

strength. The dependence between stress – cracking strain (ε_t^{ck}) in uniaxial tension and stress – crushing strain (ε_c^{in}) in uniaxial compression can be defined σ_{c0} and σ_{cu} are the compressive stress point in which nonlinear behavior initiates and the ultimate compressive strength of the concrete respectively. σ_{t0} is the tensile stress point in which non-linear behavior begins. After reaching the maximum stress, the stiffness of the concrete during unloading decreases. The rate of stiffness reduction is related to the damage of the concrete and can be determined from the multiplication of initial stiffness (E_0) to $1-d_t$ or $1-d_c$. The resulting strains followed by a reduced stiffness in zero stress point are plastic compressive strain (ε_c^{pl}) and plastic tensile strain (ε_t^{pl}) and can be calculated by Eqs. (1) to (2) (Lee and Fenves 1998)

$$\varepsilon_c^{pl} = \varepsilon_c^{in} - \frac{d_c \cdot \sigma_c}{(1-d_c) \cdot E_0} \quad (1)$$

$$\varepsilon_t^{pl} = \varepsilon_t^{ck} - \frac{d_t \cdot \sigma_t}{(1-d_t) \cdot E_0} \quad (2)$$

In these equations σ_c and σ_t are compressive and tensile strength in any points after the maximum stress. Before the maximum stress in stress-strain chart the damage is considered equal to zero. The damage after the maximum stress can be calculated from Eqs. (3) to (4).

$$d_c = \frac{\sigma_{cu} - \sigma_c}{\sigma_{cu}} \quad (3)$$

$$d_t = \frac{\sigma_{tu} - \sigma_t}{\sigma_{tu}} \quad (4)$$

The damage to the slabs under the moving load is calculated using the CDP model. The previous researches had shown the successful use of this model for concrete slabs under the impact loads (Mokhtatar *et al.* 2013).

1.2 Load transfer efficiency (LTE)

Three mechanisms of load transfer are studied in this paper. Aggregate interlock, keyway joints and dowel bars simulated in the FEM software. Load transfer efficiency (LTE) expresses the pavement joint's ability to transfer some parts of the applied load from the loaded slab to the unloaded one (Ioannides and Korovesis 1992).

Numerous researchers proposed various methods to determine the load transfer efficiency using different parameters. The most common equation to determine LTE is as follows

$$LTE_{\delta} = \frac{d_u}{d_l} \quad (5)$$

where d_u and d_l are the joint's vertical displacement in unloaded and loaded slabs, respectively and are measured at top of the joint's edge.

Teller proposed another equation to determine LTE, which is still used by researchers (Teller and Cashell 1959)

$$LTE_{\delta}^* = \frac{2d_u}{d_u + d_l} \quad (6)$$

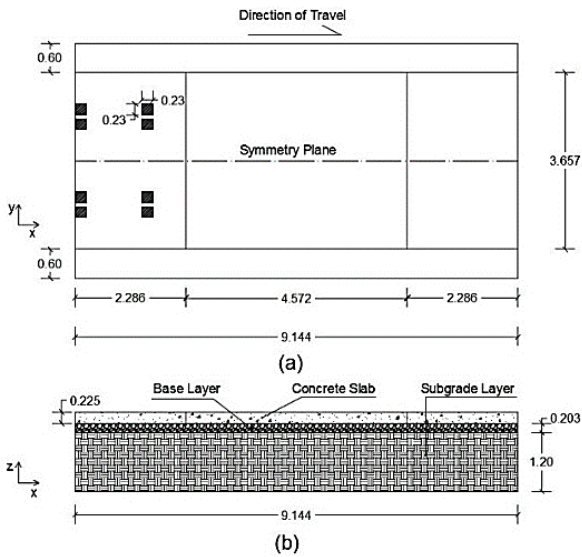


Fig. 1 3D finite-element model geometry: (a) Plan, (b) Section (in meters)

In case of joints with low load transfer ability, displacement of unloaded slabs is much lower than displacements of loaded slabs, and the transferred loads in these joints are almost zero. For joints with high load transfer ability, displacements of the slabs in both sides of the joint are close and LTE is almost equal to 1. LTE of the two aforementioned cases can be correlated using the following equation

$$LTE_{\delta}^* = 2 \times \left(1 - \frac{1}{1 + LTE_{\delta}} \right) \quad (7)$$

Since the load transfer efficiency in these cases are correlated, each one of them can be found using the other one. In this study, LTE from the first case is used to find the LTE of the joints, since it is widely used by other researchers and is also accepted by AASHTO standard (AASHTO 1993).

2. Finite-element modeling

A jointed plain concrete pavement (JPCP) similar to the experimental pavement introduced by Shoukry *et al.* (Shoukry *et al.* 1997, William and Shoukry 2001) was modeled in this study. Model included a 4.6-meter slab length that was joined to two half slabs. The pavement system includes a base layer which is placed on subgrade layer. Fig. 1 and Fig. 2 show the model and finite-element mesh used in the study. A refined mesh zone was located at the center of the joint, where wheel loads are applied, as illustrated in Fig. 2.

2.1 General description

The friction coefficient for the wheel-pavement interactions was set to 0.02. Three-dimensional reduced integration elements (C3D8R) were used for the model. The concrete slab and the base layers were assumed to be

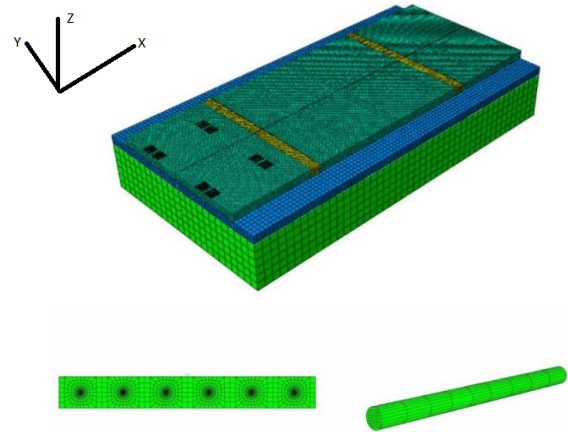


Fig. 2 3D FEM mesh (a) adjustments for the adjacent joints (b) dowel bars (c)

isotropic. Lateral sides of the concrete slab boundaries perpendicular to traffic direction are assumed to be free. Boundary condition at underneath and sides were considered fixed for the subgrade layer. Dowel-concrete interfaces as and slab-base interface are modeled using sliding interfaces with friction to enable the slab-base separation as suggested in literature (Mohamad *et al.* 2015). a friction coefficient of 1.5 simulating limited aggregate interlocking. The separating tensile forces can be initiated by inertia effects or curling of the slab. The interface between the base course and subgrade soil is assumed tied since it is unlikely that a granular base will behave as a rigid body layer that separates from the subgrade soil. To maintain the continuity of subgrade and base layers on their lateral sides and simulate the semi-infinite of soil, the boundary conditions were used as shown in Fig. 3. The 3D finite-element model was supposed to be under a load of a dump truck that is driving with 77 km/hr. For simulation of the condition that current slab is replaced with precast concrete slab, a model developed with same material properties but different load transfer systems. In the developed model, the dowel bars were removed, and the base-slab friction was reduced, which is a common practice due to implementation condition and prestressing. Three types of the load transfer systems are modeled and compared to each other; aggregate interlock, keyway joints and dowel bars. The effectiveness of each system is investigated via concrete damage plasticity and load transfer. The material properties and constants are listed in Table 1.

2.2 3D FEM model verification

Dynamic behavior of the proposed model has been validated using the Ohio Road Tests and Shoukry *et al.* numerical analysis results (Sargand and Breegle 1998, Shoukry *et al.* 2007). Studied road section was tested using cord wire-string strain gauge installed at 25.4 mm bottom and top of the concrete slabs in distances as is seen in Fig. 4 and Fig. 5. The results obtained from the pressure cells installed in 1.52 meters from the joints, and at the top of base layer were also studied to verify the finite element

Table 1 Material properties

Material	Property	Value
Concrete	Density (kg/m ³)	2400
	Compressive strength (MPa)	19.2
	Poisson's ratio	0.18
	Modulus of elasticity (MPa)	22000
Base	Density (kg/m ³)	2150
	Poisson's ratio	0.3
	Modulus of elasticity (MPa)	320
Subgrade	Density (kg/m ³)	2040
	Poisson's ratio	0.45
	Modulus of elasticity (MPa)	300
Dowel bars	Density (kg/m ³)	7800
	Poisson's ratio	0.3
	Modulus of elasticity (MPa)	2.1 × 10 ⁵

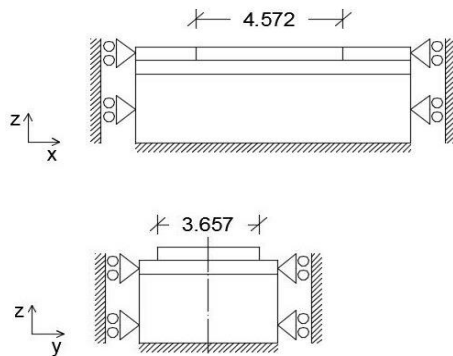


Fig. 3 Boundary conditions (in meters)

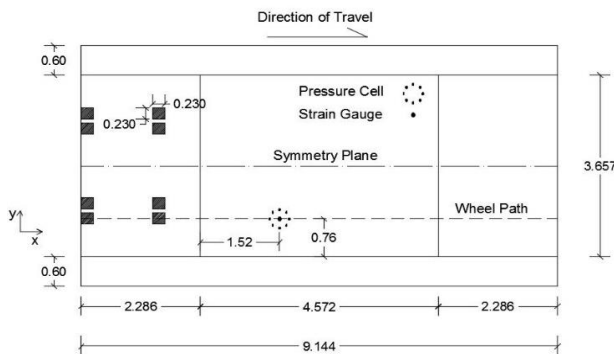


Fig. 4 Measurement locations used in Ohio road test (in meters)

model. Comparing the result from literature versus the resulted strain from the FEM model, it is shown that a good agreement existed between the results (Fig. 6).

3. Analysis and results

3.1 Load transfer via aggregate interlock

In the first model, there aren't any dowel bars or keyway joints and load transfer between adjacent slabs takes place only through aggregate interlock. This is a common practice where cast in place slabs are replaced with the precast slabs. The existing dowels are removed and load transfers via shear action of aggregates. A frictional sliding interface

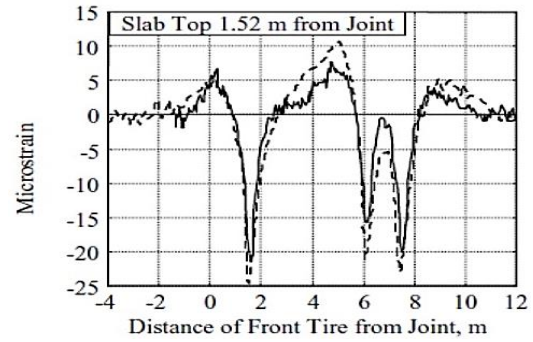


Fig. 5 Strains at top of the slab along the wheel path obtained from: (a) Ohio road test (dashed line), (b) Shoukry Model (solid line) (Sargand and Brengle 1998, Shoukry *et al.* 2007)

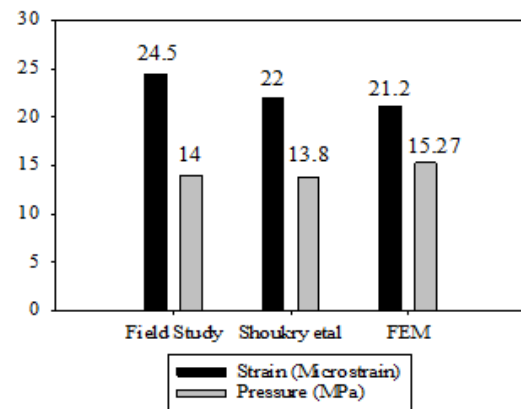


Fig. 6 Comparison of FEM results with the Ohio road tests and Shoukry model

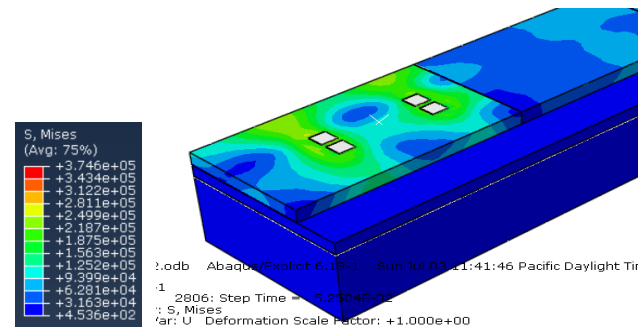


Fig. 7 Stress distribution within the slab when aggregate interlock exists at joints interface

with voids were defined that overcomes previous models in which shear spring elements were used. Fig. 7 shows stress diagrams of the slabs where the axle load is placed on the left slab. As it is clear, only some of the stresses are transferred to the adjacent slab due to aggregate interlock.

Frictional behavior is applied to the slabs interface to simulate aggregates interlock. A range of friction coefficients (μ) are assigned to the side interface along the transverse joint to simulate the sliding interface with voids and friction therefore, 0.02, 0.1, 0.7 and 1.5 were selected as the friction coefficient at joints interface. Two elements on mid-top of the first and approaching slab are selected to gain further insights. The tensile stresses of the selected

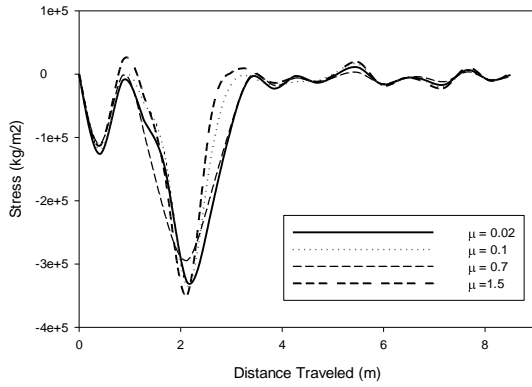


Fig. 8 Tensile stress at mid-point of the first slab

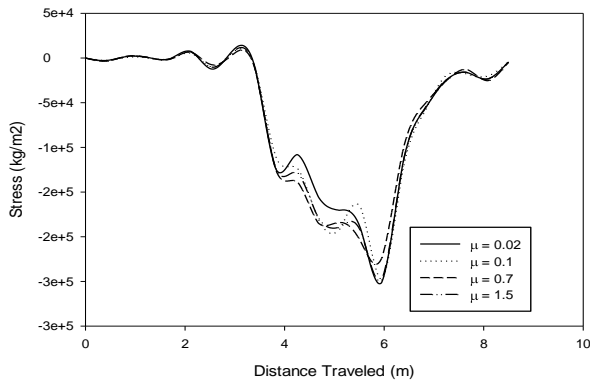


Fig. 9 Tensile stress at the mid-point of the second slab

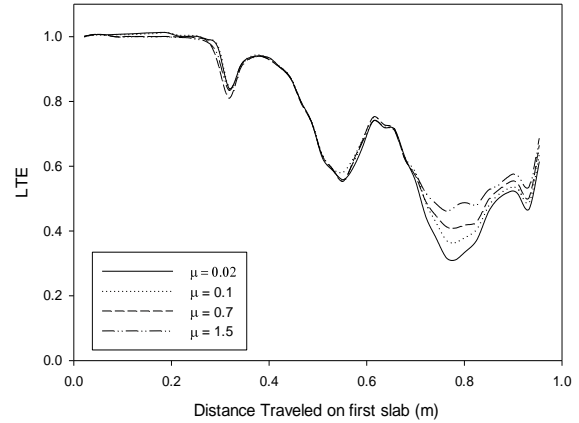


Fig. 10 LTE between the slabs when only aggregate interlock exists at the joints interface

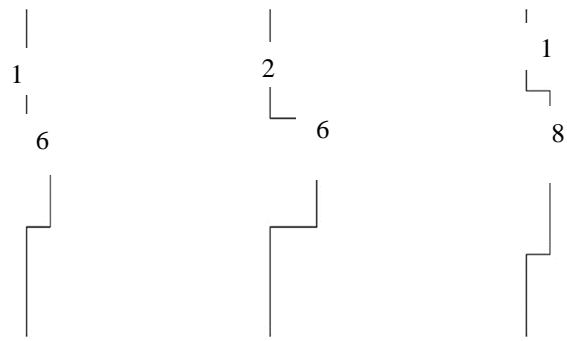


Fig. 11(a) Types of the keyway joints used in the FEM

element are shown on Figs. 8 and 9.

The abscissa shows the distance that axle load traveled on the slab. The result proved that even the high aggregate interlock is not effective on the stress distribution within the pavements. It also shows that the maximum tensile stress occurs under the tires and decreases as axle moves away from the loaded area. Fig. 10 shows the LTE where the axle load is moved on the undoweled pavement. The graph is depicted for the element under the wheel load. The numerous analyses show that the computed LTE for other points, including side of the edge or under the first wheel or between the wheels are almost similar, but the LTE under the wheel load was slightly lower. When the axle load moves to the joints, the LTE starts to decrease. The rate of decreasing LTE is lower where a stronger interlock aggregate interlock exists. The LTE is not acceptable when the load reaches to slab joints causing a significant drop in load transfer.

3.2 Keyway joints

It was shown that the load on the first slab is not transferred completely via aggregate interlock, especially when the wheel loads are near the joints. The keyway joints, as introduced later, are a type of load transfer system embedded in some of the precast pavements. The keyway joints were modeled to investigate the load transfer through this type of joints. The keyway joints are modeled using 8-node solid brick elements.

Sliding interface of the joint were defined using surface



Fig. 11(b) schematic of the keyed joint

to surface frictional elements. Results shown that the load transfer was improved compared to aggregate interlock. Three types of keyway joint are studied in the FEM model. The tongue and groove of the keyway are designed with different dimensions. 6×1 6×2 and 8×1 cm were selected for the tongue and groove as illustrated in Fig. 11.

These types of the joints were selected to study the effects of the tongue and groove dimension on the load transfer. The effects of the keyway joints on the developed stresses within the first and second slabs are shown in the Fig. 12 and Fig. 13 respectively. The results shown that this type of the connections was effective on the induced stresses but the differences between these models were not significant. The FEM showed that keyway joints significantly reduced tensile stresses developed at the mid-slab.

Keyway joints improved load transfer compared to aggregate interlock. As shown in Fig. 14 the stresses are

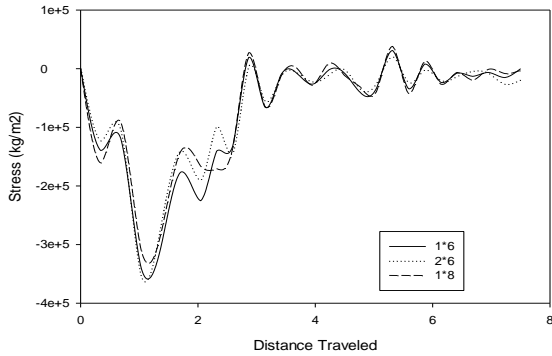


Fig. 12 Tensile stress in the middle of the first slab

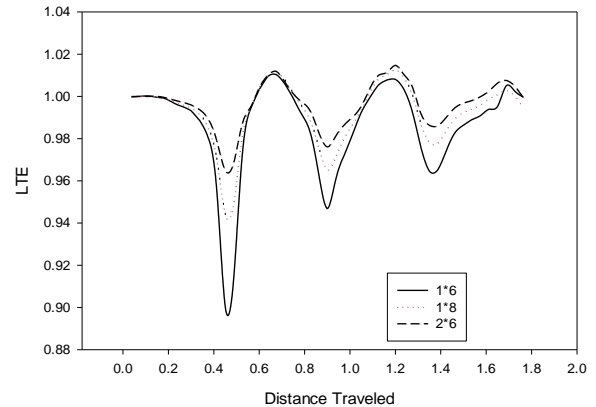


Fig. 15 LTE for the keyway joints with different tongue and groove design

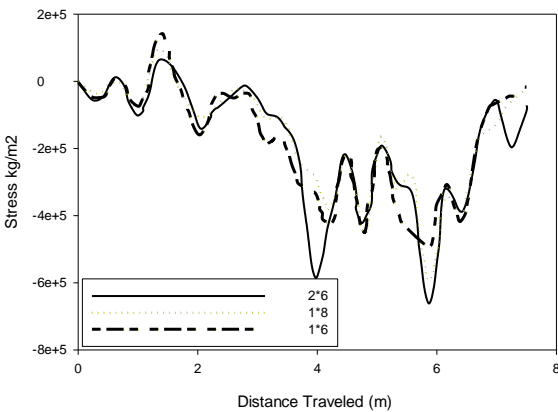


Fig. 13 Tensile stress in the middle of the second slab

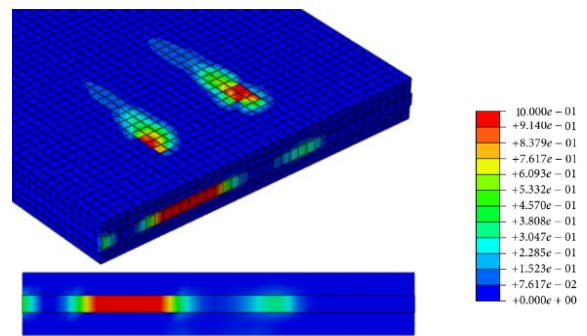


Fig. 16 Compressive damage in the 1x6 keyway joint (tongue)

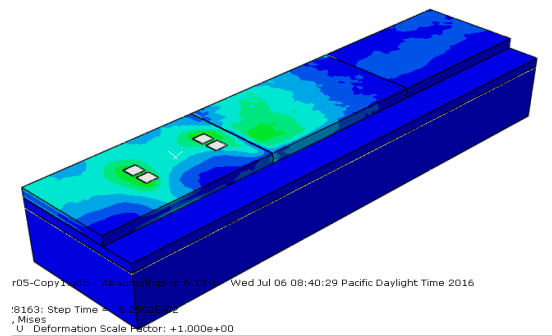


Fig. 14 Stress distribution within the pavement with keyway joints

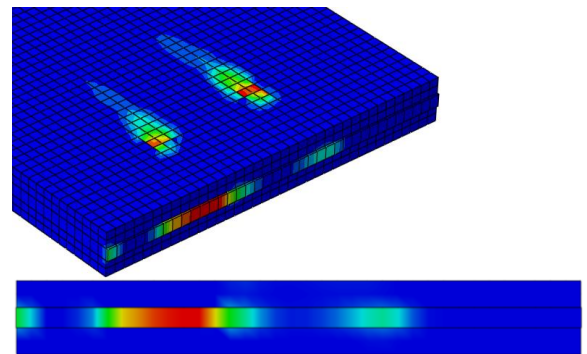


Fig. 17 Compressive damage in the 1x8 keyway joint (tongue)

transferred to the adjacent slab, also the tensile stresses developed along the transverse joints are reduced. Compared to Fig. 7 load transfer in keyway joints is more efficient than aggregate interlock. The second joint is modeled using aggregate interlock so that the stresses are not transferred to third slab efficiently.

The effects of the different design for the tongue and groove on the LTE are plotted against the distance traveled and shown in the Fig. 15. The results indicate that the keyway performed its intended function in transferring the load across the joint. Increasing the thickness of the tongue the LTE was increased. With increasing the height of the tongue the LTE was decreased so a limit must be considered for the key way joints. Further analyses were performed to investigate the effect of the friction between the tongue and groove, and they showed that the friction

was not effective on the total response of the keyway joints.

3.3 Plastic damage

The structural distresses produced by stress concentrations and excessive stresses in the transverse joints was also studied by the authors. This information cannot be provided by experimental investigations and analytical models and results will provide a better understanding of the stresses, and the distress (damage) produced due to substantial loadings in the pavement slabs. The concrete damage plasticity model is very versatile and capable of predicting the behavior of concrete structures subjected to monotonic, cyclic and/or dynamic loading. The

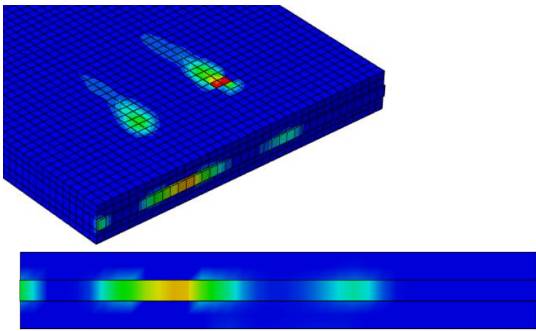


Fig. 18 Compressive damage in the 2x6 keyway joint (tongue)

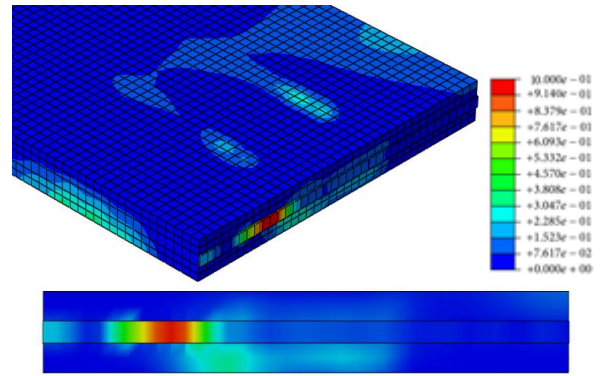


Fig. 20 Tensile damage distribution in the 1x6 model

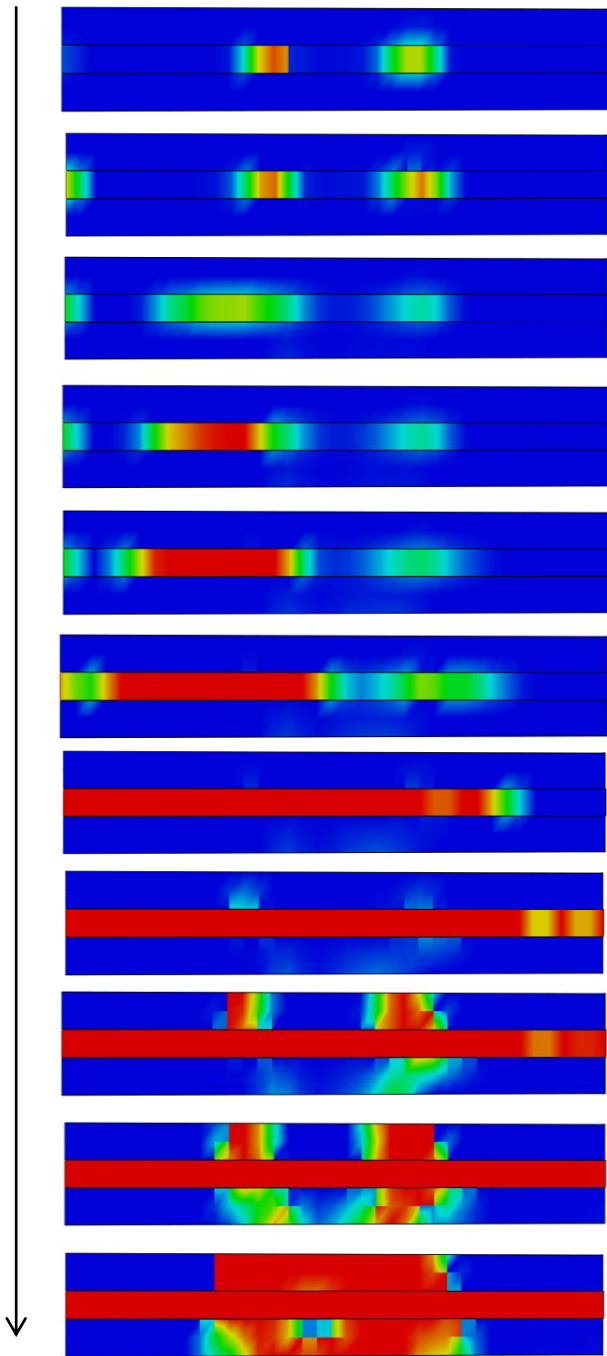


Fig. 19 The spread of the compressive damage on the keyway joints (tongue)

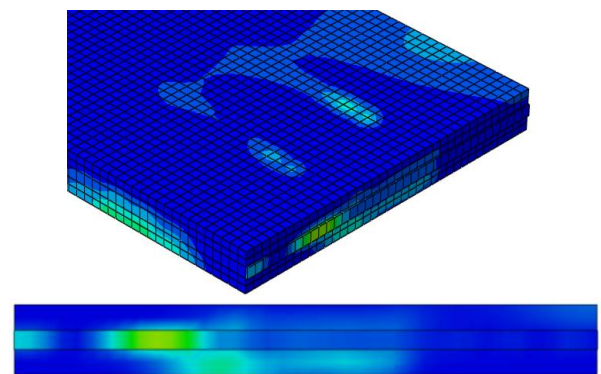


Fig. 21 Tensile damage distribution in the 1x8 model

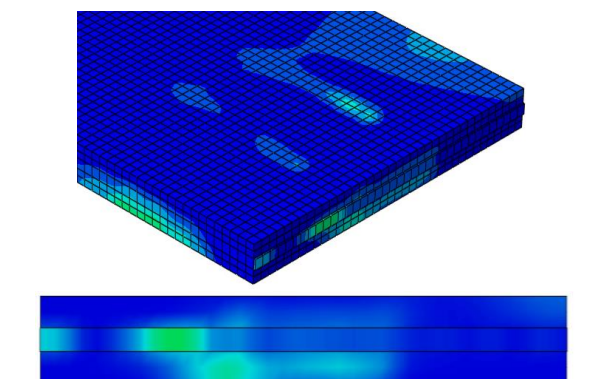


Fig. 22 Tensile damage distribution in the 2x6 model

concrete undergoes compressive and tensile damages when a heavy wheel load traversed on the slab. In the current study, the axle loads were increased three times to assess the damage in the keyway joints. The tensile damage causes the concrete to develop cracking, which severely reduces the bearing capacity of the concrete. Compressive damage is accompanied by the crushing of the slab. This paper aims to determine which damage type is crucial in the keyway joints because it has significant effects on the load transfer between joints.

Figs. 16-18 show the compressive damage pattern for the 6x1 cm and 8x1 cm and 6x2 cm models. The red color indicates the complete compressive damage or total crush of the element. Damage spread is almost similar in the models, but the amount of the damage is different. In all the finite-element models, the damage caused by inner wheels is more

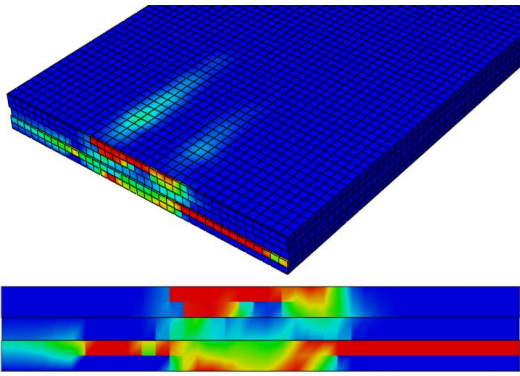


Fig. 23 The compressive damage in the keyway groove (1×6)

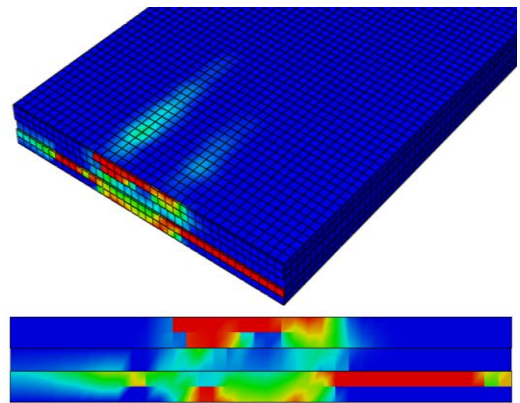


Fig. 24 The compressive damage in the keyway groove (1×8)

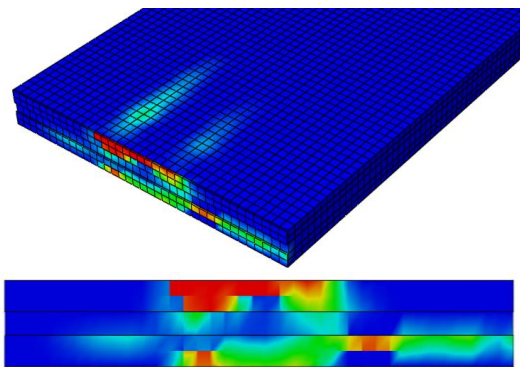


Fig. 25 The compressive damage in the keyway groove (2×6)

than outer wheels, and the edge of the road is less damaged. The damage in the joints is mostly caused by inner wheels. The 1×6 model is damaged the most, and the damage to the 2×6 model was less than the 1×8 model. The reason might be the higher interaction of the tongue and groove.

Fig. 19 shows the distribution of the compressive damage at the joint edge. The damage starts from underneath of the axle load. The inner wheel load is heavier and causes more damage under it. After spreading to the whole edge, the compressive damage reaches to slab.

The cracking probability in the slab is shown by tensile damages. The results shown that the tensile damage in the keyway joint is less than compressive damage. Figs. 20-22

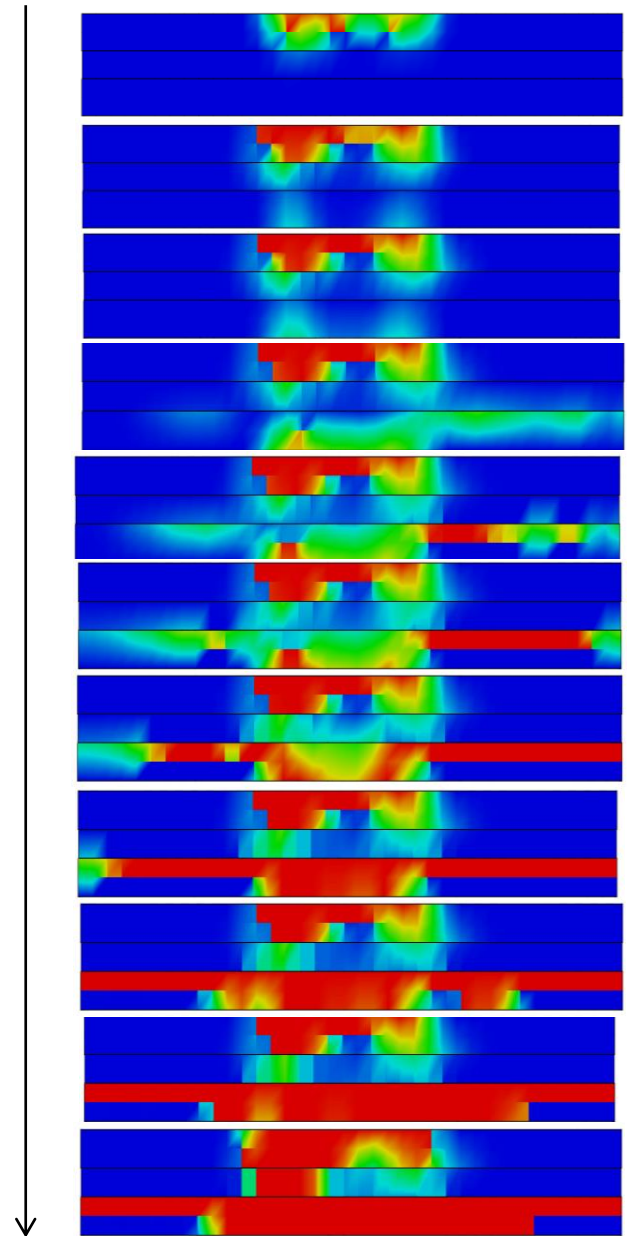
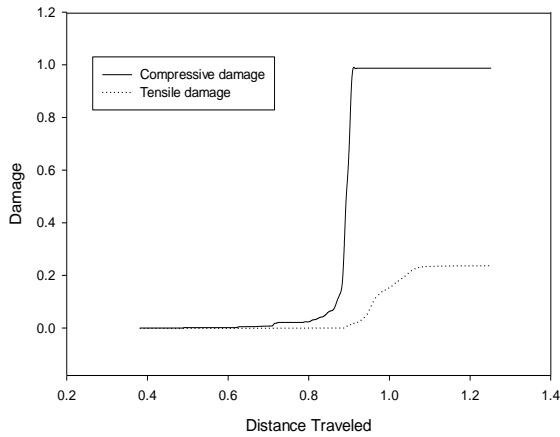


Fig. 26 The compressive damage spread in the keyway groove

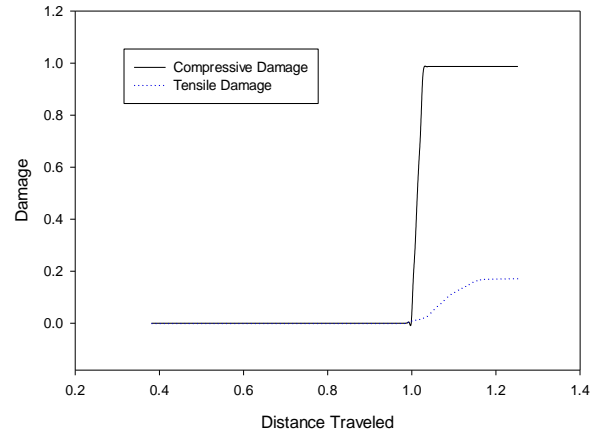
show the tensile damage for all the models. The maximum damage to an element was 0.2, far from 1 for an element to crack. The results prove that for the design of the keyway joints, the compressive damage is more important than tensile damage.

As it was shown, the 1×6 was the most damaged model, and the least damage was observed in the 2×6 model. Investigating compressive damage shown that, the slab will not face compressive damage until joint crushes. However, when dealing with cracking one should notice that the slab itself will face tensile damage with the keyway system.

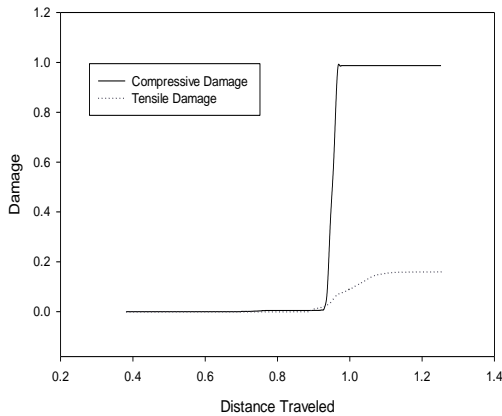
The keyway groove will also face compressive damage. Figs. 23 to 25 show the compressive damage distribution in the keyway groove. The results show that the compressive damage was mostly effective on top and bottom of the groove. Comparing 1×6 and 1×8 models shows that the



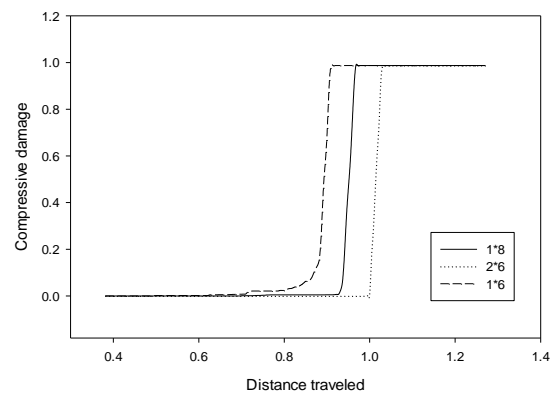
1x6



2x8



1x8



compressive damages in all models

Fig. 27 The numerical scheme of damages to slab joints

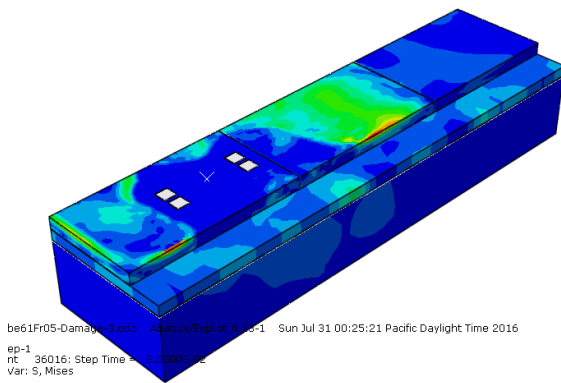


Fig. 28 Stress distribution within doweled slab

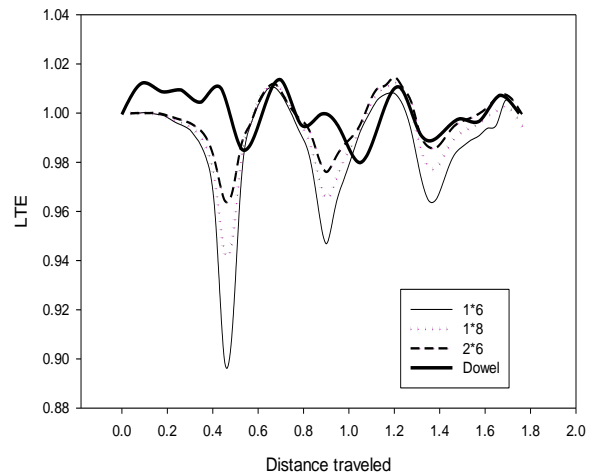


Fig. 29 Comparison of doweled system with keyway joints

damage to 1x8 was more than the 1x6 model due to the difference in the opening. The 2x6 shows the least damage.

Damage spread in the groove is shown in Figure 26. The damage started underneath the wheel load, and it was higher under the inner wheel. With increasing the load, the damage to the bottom of the groove increased and developed and began to spread to the slab.

In order to compare models numerically, the damage for critical location, the element on the keyway tongue under the inner wheel load was selected. The previous results showed that the highest damage to the keyway system occurs here.

Fig. 27 shows the damage to selected element in the FEM. The damage is plotted against the distance traveled. As it is clear, the compressive damage is higher than the tensile damage, and should be considered during the keyway design. Comparing the compressive damage in the models shown that even though all models are crushed after passage of the heavy load, but the 1x6 model damaged first, and the damage spread was slower in the 2x6 model. The results shown that the keyway joints performance is

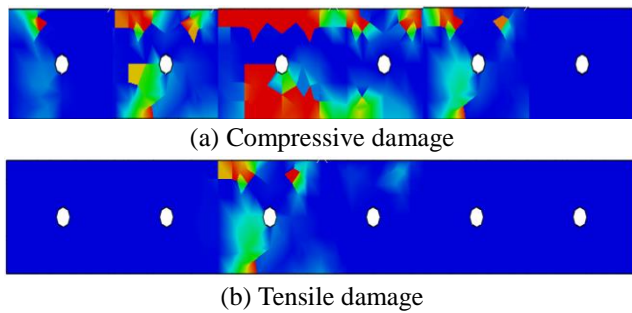


Fig. 30 Damage spread in doweled joint

superior than the aggregate interlock for load transfer and reducing induced stresses.

The performance of the systems is compared with joints with dowel system. Load transfer is only through dowel bar interaction. A separate model was developed with six equally spaced dowels. The dowel length is 46 cm and 4 cm diameter. Slippery condition is considered for dowel-concrete interface at the unloaded side and full contact is assumed with the concrete slab on the loaded side.

The Fig. 28 shows that the stresses are transferred to the adjacent slab efficiently when dowels are embedded within the model. LTE for the model with dowels are compared with the keyway system and presented in Fig. 29. The results showed that the dowels had the highest LTE.

In this model, the load implied is the common load that slabs encounter the concrete doesn't go to the plastic range and so the wheel load for the further analysis increased three times.

The rate of the damage spread is investigated and shown in Fig. 30. The result shown that the compressive damage is higher at the joints. The damage is higher under the wheel load, and the load is mostly carried by third dowel. The damage to surrounding concrete at the side dowel is least. In case of the tensile damage only a small portion of concrete is close to cracking, and almost all other areas remain intact.

The colored red element is a demonstration of the total damage, showing the compressive damage is higher. Compared to other load transfer methods, the dowel controlled the amount of damage to the surrounding concrete. The amount of damage at a certain point of the first slab joint interface is investigated. The point under the third dowel which is under the wheel path is chosen to compare damages numerically. Fig. 31 shows that tensile damage occurs sooner than compressive damage, but the rate remains constant. Then the compressive damage increases significantly and become the major form of distress under the dowels.

4. Conclusions

Precast concrete pavement systems are used in highways with high traffic volume and where lane closures are challenging. Pavement performance is mainly affected by joint load transfer condition. There are a few techniques to ensure effective load transfer at transverse joints. The 3D

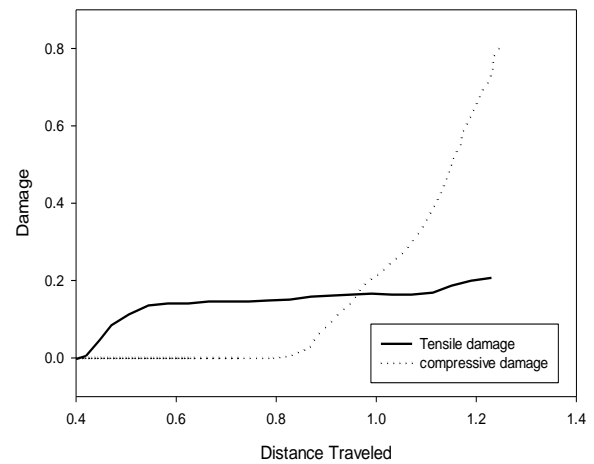


Fig. 31 The numerical scheme of damages to doweled slab joints

finite-element models were developed for precast concrete slabs intended for repair of the existing concrete pavements with transverse joints. The pavements were supported by a base, sub-base and sub-grade layers. Three types of transverse joints which are used in practice, were developed and compared. The slabs were first subjected to normal 80 kN axle load to demonstrate the stress distribution in the slabs. A 240 kN heavy load was passed on the road to investigate the damage pattern in the slab joints. The results showed that:

- Only some of the stresses are transferred to the adjacent slab due to aggregate interlock and even increasing the aggregate interlock is not helpful on the stress distribution within the pavements. The LTE is not acceptable when the load reaches to slab joints. When the cast in place slabs at transverse joints are replaced with the precast pavements, the joints should not rely on aggregate interlock for load transfer.
- The load transfer by using keyway joints was improved compared to aggregate interlock. The panel on one side of the joint has the keyway tongue, and the panel on the other side has the keyway groove. The FEM showed that keyway joints significantly reduced tensile stresses developed at the mid-slab. Increasing the thickness of the tongue the LTE was increased. With increasing the height of the tongue the LTE was decreased so a limit must be considered for the key way joints. The damage to the joints is mostly caused by inner wheels. The predominant damage type is compressive damage. The 1×6 model is damaged the most, and the damage to the 2×6 model was less than 1×8 model.
- Stresses are transferred to the adjacent slab efficiently when dowels are embedded in the model. When the axle load approaches joints, tensile damage occurs sooner than compressive damage, but the rate remains constant. Then the compressive damage increases significantly and become the major form of distress under the dowels. The slots for the dowels should cut in the precast slab or existing pavement since this is the best system for transferring loads to adjacent slab.

References

- AASHTO, G. (1993), Guide for Design of Pavement Structures, American Association of State Highway and Transportation Officials, Washington, DC.
- Abo-Qudais, S.A. and Al-Qadi, I.L. (2000), "Dowel bars corrosion in concrete pavement", *Can. J. Civil Eng.*, **27**(6), 1240-1247.
- Ashtiani, R.S. and De Haro, G. (2016), "Temperature sensitivity of precast concrete panels used for the repair of rigid pavements", *International Conference on Transportation and Development*.
- Channakeshava, C., Barzegar, F. and Voyiadjis, G.Z. (1993), "Nonlinear FE analysis of plain concrete pavements with doweled joints", *J. Tran. Eng.*, **119**(5), 763-781.
- de Larrard, F., Sedran, T. and Balay, J.M. (2013), "Removable urban pavements: an innovative, sustainable technology", *Int. J. Pav. Eng.*, **14**(1), 1-11.
- Gopalaratnam, V., Davis, B.M., Dailey, C.L. and Luckenbill, G.C. (2007), *Performance Evaluation of Precast Prestressed Concrete Pavement*.
- Hesami, S. and Sadeghi, V. (2015), "Numerical investigation of the shape memory alloy dowels in jointed concrete pavements", *Int. J. Pav. Res. Technol.*, **8**(4), 251.
- Ioannides, A.M. and Korovesis, G.T. (1992), "Analysis and design of doweled slab-on-grade pavement systems", *J. Tran. Eng.*, **118**(6), 745-768.
- Kim, J. and Hjelmstad, K.D. (2003), "Three-dimensional finite element analysis of doweled joints for airport pavements", *Tran. Res. Record: J. Tran. Res. Board*, **1853**(1), 100-109.
- Lee, J. and Fenves, G.L. (1998), "Plastic-damage model for cyclic loading of concrete structures", *J. Eng. Mech.*, **124**(8), 892-900.
- Littleton, P. and Mallela, J. (2014), *Florida Demonstration Project: Precast Concrete Pavement System on US 92*.
- Merritt, D.K. (2000), "The feasibility of using precast concrete panels to expedite highway pavement construction", Center for Transportation Research, University of Texas at Austin.
- Mohamad, M.E., Ibrahim, I.S., Abdullah, R., Rahman, A.B. Abd, Kueh, A.B.H. and Usman, J. (2015), "Friction and cohesion coefficients of composite concrete-to-concrete bond", *Cement Concrete Compos.*, **56**, 1-14.
- Mokhtar, S., Abdullah, R. and Kueh, A. (2013), "Computational impact responses of reinforced concrete slabs", *Comput. Concrete*, **12**(1), 37-51.
- Nejad, F.M., Ghafari, S. and Afandizadeh, S. (2013), "Numerical analysis of thermal and composite stresses in prestressed concrete pavements", *Comput. Concrete*, **11**(2), 169-182.
- Peng, P., Wu, D.F., Tian, B. and Niu, K.M. (2014), *Precast Pavement Smoothness Control Method, Applied Mechanics and Materials*, Trans Tech Publ.
- Priddy, L.P., Bly, P.G., Jackson, C.J. and Flintsch, G.W. (2014), "Full-scale field testing of precast Portland cement concrete panel airfield pavement repairs", *Int. J. Pav. Eng.*, **15**(9), 840-853.
- Priddy, L.P., Pittman, D.W. and Flintsch, G.W. (2014), "Load transfer characteristics of precast Portland cement concrete panels for airfield pavement repairs", *Tran. Res. Record*, **2456**, 42-53.
- Sadeghi, V. and Hesami, S. (2017), "Investigation of load transfer efficiency in jointed plain concrete pavements (JPCP) using FEM", *International Journal of Pavement Research and Technology*.
- Sargand, S. and Breegle, D. (1998), "Three-dimensional finite element software development and verification case study", *First National Symposium of 3D Finite Element for Pavement Analysis and Design*.
- Shoukry, S., Martinelli, D. and Reigle, J. (1997), "Universal pavement distress evaluator based on fuzzy sets", *Tran. Res. Record: J. Tran. Res. Board*, **1592**, 180-186.
- Shoukry, S.N., Fahmy, M., Prucz, J. and William, G. (2007), "Validation of 3DFE analysis of rigid pavement dynamic response to moving traffic and nonlinear temperature gradient effects", *Int. J. Geomech.*, **7**(1), 16-24.
- Shoukry, S.N., William, G. and Riad, M. (2002), "Characteristics of concrete contact stresses in doweled transverse joints", *Int. J. Pav. Eng.*, **3**(2), 117-129.
- Smadi, M. and Belakhdar, K. (2007), "Nonlinear finite element analysis of high strength concrete slabs", *Comput. Concrete*, **4**(3), 187-206.
- Tayabji, S. (2015), *Precast Concrete Pavement Implementation by US Highway Agencies*.
- Tayabji, S. and Hall, K. (2008), *Precast Concrete Panels for Repair and Rehabilitation of Jointed Concrete Pavements*, CPTP TechBrief.
- Tayabji, S., Ye, D. and Buch, N. (2013), *Precast Concrete Pavement Technology*, Transportation Research Board.
- Teller, L.W. and Cashell, H.D. (1959), *Performance of Doweled Joints under Repetitive Loading*, Highway Research Board Bulletin.
- William, G.W. and Shoukry, S.N. (2001), "3D finite element analysis of temperature-induced stresses in dowel jointed concrete pavements", *Int. J. Geomech.*, **1**(3), 291-307.

CC